Journal of Biomechanics 48 (2015) 779–786

Contents lists available at ScienceDirect

Journal of Biomechanics

journal homepage: www.elsevier.com/locate/jbiomech
www.JBiomech.com

Toward patient-specific articular contact mechanics

Gerard A. Ateshian [a], Corinne R. Henak [b], Jeffrey A. Weiss [c]

[a] Department of Mechanical Engineering, Columbia University, New York, NY 10027, USA
[b] Department of Biomedical Engineering, Cornell University, Ithaca, NY 14850, USA
[c] Department of Bioengineering, Department of Orthopaedics, and Scientific Computing and Imaging Institute, University of Utah, Salt Lake City, UT 84112, USA

ARTICLE INFO

Article history:
Accepted 26 November 2014

ABSTRACT

The mechanics of contacting cartilage layers is fundamentally important to understanding the development, homeostasis and pathology of diarthrodial joints. Because of the highly nonlinear nature of both the materials and the contact problem itself, numerical methods such as the finite element method are typically incorporated to obtain solutions. Over the course of five decades, we have moved from an initial qualitative understanding of articular cartilage material behavior to the ability to perform complex, three-dimensional contact analysis, including multiphasic material representations. This history includes the development of analytical and computational contact analysis methods that now provide the ability to perform highly nonlinear analyses. Numerical implementations of contact analysis based on the finite element method are rapidly advancing and will soon enable patient-specific analysis of joint contact mechanics using models based on medical image data. In addition to contact stress on the articular surfaces, these techniques can predict variations in strain and strain through the cartilage layers, providing the basis to predict damage and failure. This opens up exciting areas for future research and application to patient-specific diagnosis and treatment planning applied to a variety of pathologies that affect joint function and cartilage homeostasis.

In memory of Dr. Rik Huiskes

It is with great fondness that I recall my interactions with Dr. Rik Huiskes, starting from the very early years of my doctoral training in the late 1980s. I had joined the Orthopaedic Research Laboratory of Dr. Van C. Mow as a doctoral student in 1986, soon after his move from Rensselaer Polytechnic Institute to Columbia University. In my first interview with Dr. Mow, he had outlined one of the research projects I ended up working on, which focused on characterizing the three-dimensional topography of articular surfaces using stereophotogrammetry. Upon joining the lab, he asked me to read the paper by Huiskes et al. (1985), titled "Analytical stereophotogrammetric determination of three-dimensional knee-joint geometry" to get started on this project. He explained that he had visited Dr. Huiskes at the University of Nijmegen and had been extremely impressed by this methodology, which he wanted to replicate in his new laboratory. Together with my friend and co-graduate student Louis J. Soslowsky, we labored over this effort relentlessly, poring over the paper and teasing out every possible detail to help us replicate this system, both with hardware and software. Dr. Huiskes visited our lab in New York City soon after we started this project and it was with great excitement that I first met the person behind the scientific paper. This first encounter was quite memorable to me as a young student; over time I got to know Dr. Huiskes much better personally, as I benefited from his close friendship with Dr. Mow, which translated into increased encounters over the years. I felt extremely honored when Dr. Huiskes sent me my first manuscript to review, for the Journal of Biomechanics, when I became an Assistant Professor. Over the years, Rik imparted much wisdom to me, both professionally and personally, and I always looked forward to the opportunity of seeing him at conferences and other venues. I was always impressed by the quality and impact of his research and followed his work closely. I developed a kinship with several of his former students, most notably Leendert Blankevoort, who spent a year at Columbia as a visiting scholar and became a good friend. Dr. Huiskes' legacy is all around us and it was my great privilege to have known him and interacted with him over many years. *GAA*.

1. Introduction

Articular cartilage is the connective tissue that lines the ends of bones in diarthrodial joints. Cartilage serves as the bearing material whose primary function is to cushion the load transmission across joints while minimizing friction. Adult articular cartilage is avascular and exhibits a limited ability to repair. Consequently, cartilage degeneration occurs when the tissue's mechanical or biochemical environment significantly deviates from normal conditions, as in

http://dx.doi.org/10.1016/j.jbiomech.2014.12.020
0021-9290/

injury, or when the tissue's metabolism can no longer keep up with the normal wear and tear of daily activities, as in aging. Articular contact mechanics has long been a topic of interest in the joint biomechanics literature; a better understanding of the load-bearing function of cartilage in relation to the tissue's structure is expected to yield significantly greater insights into the pathomechanics of joint degeneration and the treatment modalities that aim to repair or replace this tissue with engineered equivalents.

A number of challenges have confronted investigators in their efforts at characterizing contact mechanics in diarthrodial joints. At a fundamental level, the material response of articular cartilage had to be properly characterized to produce experimentally validated constitutive relations that could describe its response to various loading conditions. The contact interface conditions had to be elucidated from experiments and theory. Where possible, analytical solutions of cartilage contact mechanics had to be developed that could yield fundamental insights with regard to load support and the dependence of tissue strains and stresses on contact interface tractions. Computational contact methods had to be formulated, implemented, verified against analytical solutions and validated against experimental results. Quantification of the anatomical topography of articular layers had to be performed to provide geometric models as input to computational analyses. Finally, the integration of other soft and hard tissue structures into those models has been required to produce more realistic models of whole joints.

Many of these challenges have been substantially addressed and met, though opportunities for further refinements in the modeling approach and more substantive validations of whole-joint response against experimental data remain active areas of investigation. This article reviews some of the salient milestones in cartilage contact mechanics and presents a few of the latest developments in relation to computational contact analyses. The strategies and major technical hurdles associated with three dimensional patient-specific analysis of contact mechanics are discussed, with special attention to geometry acquisition in vivo. The application of patient-specific computational analysis is described in relation to studies of the hip. Finally, we present important areas that require further research and future directions. The reader is referred to textbooks for details on the composition and structure–function relationships of articular cartilage (Freeman, 1979; Mow and Huiskes, 2005).

2. Cartilage material response and constitutive relations

2.1. Viscoelasticity and tension–compression nonlinearity

When subjected to extended durations of loading, articular cartilage does not behave as an elastic material, as reported by Elmore et al. in their classic article titled "Nature of 'imperfect' elasticity of articular cartilage" (Elmore et al., 1963). Extensive characterizations of the time-dependent response of cartilage to loading was reported by Hayes and Bodine (1978) and Hayes and Mockros (1971) who described this tissue as 'viscoelastic'. Hayes and Bodine (1978) specifically alluded to the fact that cartilage viscoelasticity could result from flow-dependent as well as flow-independent mechanisms, the former alluding to the frictional interactions of the interstitial fluid with the porous collagenous matrix, and the latter alluding to intrinsic viscoelasticity of the solid matrix. This distinction has persisted over the years, with various investigators giving more or less weight to either mechanism.

To describe the flow-dependent viscoelasticity of cartilage, Mow et al. (1980) adopted the framework of mixture theory (Bowen, 1976, 1980) to model the tissue as a biphasic material consisting of an intrinsically incompressible porous solid matrix and interstitial fluid. This framework emphasized the importance of interstitial fluid pressurization and flow within the deformable porous matrix, leading to loss of tissue volume as a result of fluid exudation. They modeled the solid matrix as compressible isotropic elastic, where the compressibility arises from its porous nature. Validations from experimental measurements of tissue deformation and interstitial fluid pressure were performed in confined compression creep, stress-relaxation, and dynamic loading (Ateshian et al., 1997; Holmes et al., 1985; Mow et al., 1980; Soltz and Ateshian, 1998, 2000b).

To capture the experimental response of cartilage in unconfined compression however, it became necessary to account for the distinctively stiffer stress–strain response of cartilage in tension than compression noted from experiments (Armstrong and Mow, 1982; Huang et al., 2005; Kempson et al., 1968), as confirmed from several theoretical and experimental studies (Armstrong et al., 1984; Brown and Singerman, 1986; Cohen et al., 1998; Park et al., 2003; Soltz and Ateshian, 2000a; Soulhat et al., 1999). Further improvement was observed between experiments and theory when the solid matrix was modeled with multiple or continuous tensile-bearing fibril distributions (Ateshian et al., 2009; Wilson et al., 2004).

As an alternative to accounting for cartilage's tension–compression nonlinearity, some studies proposed that the intrinsic viscoelasticity of the solid matrix was a dominant mechanism needed to describe its response to unconfined compression (DiSilvestro et al., 2001a, 2001b). However, subsequent theoretical and experimental investigations suggested that flow-dependent viscoelasticity was the dominant dissipative mechanism in cartilage (Huang et al., 2001, 2003; Park and Ateshian, 2006; Park et al., 2004).

2.2. Osmotic swelling

The articular cartilage matrix consists primarily of a type II collagen fibrillar matrix and aggregating proteoglycans (aggrecans). At physiological pH these proteoglycans are negatively charged, attracting cations and repelling anions such that the interstitial fluid osmolarity increases substantially above that of the tissue's bathing environment. This osmotic disparity causes an influx of water that swells the tissue; since the swelling is resisted by the fibrillar matrix, an osmotic pressure arises to counter this matrix stress (Basser et al., 1998; Maroudas, 1968). This phenomenon is called the Donnan effect and the resulting pressure is the Donnan osmotic pressure.

The Donnan effect has been modeled in articular cartilage with the triphasic theory (Lai et al., 1991) by extending the mixture framework to include two monovalent counter-ions in the interstitial fluid as well as a charge density fixed to the solid matrix to represent proteoglycan charge. In addition to predicting osmotic swelling, this framework also models the electric potential and current density in the tissue, in response to mechanical, chemical or electrical loading conditions. Other investigators subsequently developed conceptually similar models with charged or neutral solutes (Gu et al., 1998; Huyghe and Janssen, 1997; Mauck et al., 2003; Wilson et al., 2005).

3. Analytical contact solutions

Cartilage forms a layer of soft tissue anchored to a much stiffer subchondral bone plate and trabecular bone substrate. The contact area between the opposing articular layers of a joint has a characteristic length typically greater than the layer thickness. Therefore, analytical solutions for cartilage contact cannot be based directly on Hertz contact theory, which models the contacting materials as half-spaces where the contact size is small compared to the typical dimensions of the contacting bodies (Johnson, 1985). Instead, the most elementary assumption is to model the cartilage as an elastic layer bonded to a rigid foundation.

The first exact theoretical contact analysis widely used in cartilage mechanics was the indentation analysis by Hayes et al. (1972), which provided solutions for indentation of an isotropic linear elastic layer with a frictionless plane-ended cylindrical or spherical indenter. Even though the analysis could have been used to examine more closely the state of strain and stress in contacting articular layers, it was applied mostly to extract cartilage material properties from indentation measurements.

Armstrong used his insights from biphasic theory (Armstrong et al., 1984) to propose approximate plane strain elastic contact solutions for a thin layer of cartilage in the limits of instantaneous and equilibrium responses (Armstrong, 1986). For the instantaneous response, cartilage was assumed to behave as an incompressible isotropic linear elastic material, since the interstitial fluid cannot exude instantaneously from the tissue upon loading. For the equilibrium response, cartilage was modeled as a compressible isotropic linear elastic material, given that the loss of interstitial fluid is accompanied by reduction of the pore volume. The greatest shear stress in the instantaneous response occurred at the cartilage–bone interface, beneath the location where the articular contact pressure gradient was greatest, consistent with experimental observations (Meachim and Bentley, 1978). Also, the equilibrium response exhibited significantly lower contact pressure, as the contact area spread more widely under the same load.

The analytical foundations of Hayes' study were later used by Eberhardt et al. (1990, 1991a, 1991b) to formulate contact analyses of layered elastic spheres for the specific purpose of examining articular contact mechanics. The underlying bone was also modeled as an elastic layer. Isotropic linear elastic models were employed for cartilage, using Poisson ratios approaching the incompressibility limit, justified by previous theoretical findings (Armstrong et al., 1984). They also confirmed that large shear stresses could be observed at the cartilage–bone interface, consistent with experimental findings of damage at that location in osteoarthritic joints. They did not observe significant tensile stresses in the articular layer, a surprising outcome considering the prevalence of surface clefts in osteoarthritic joints. They reported negligible influence of the bone deformation on the cartilage response.

A biphasic contact analysis was subsequently reported (Ateshian et al., 1994) which incorporated Armstrong's thin layer approximation into the biphasic framework to produce an asymptotic solution of the short-term response of contacting spherical biphasic layers. This contact analysis, which modeled the solid matrix as isotropic linear elastic, distinguished between the fluid pressure and solid matrix stress contributions to the total stress, showing that interstitial fluid pressurization contributed most of the contact stress in the early time response. As a result, solid matrix stresses were significantly smaller than the total stresses predicted from equivalent incompressible elastic analyses. Under a constant load, loss of fluid pressurization would only become significant after $\sim$200 s, based on representative cartilage material properties and the congruence of the contacting surfaces. Similar to earlier models, this biphasic analysis also predicted elevated shear stresses at the cartilage–bone interface with no excessive tensile solid stresses near the articular surface. The findings of this asymptotic thin-layer analysis were later reinforced by a more general analytical solution of the transient biphasic contact response (Kelkar and Ateshian, 1999).

A subsequent contact analysis of continuously rolling or sliding cylindrical biphasic layers demonstrated that interstitial fluid pressurization could sustain more than 90% of the contact load indefinitely, as long as the velocity of the migrating contact pressure significantly exceeded the characteristic velocity of interstitial fluid flow in the tissue (Ateshian and Wang, 1995). Taken together, these biphasic contact analyses suggested that normal physiologic articular joint contact conditions did not necessarily produce significant loss of interstitial fluid pressurization under activities of daily living.

4. Computational contact algorithms

Some of the earliest computational joint contact analyses (Brown and DiGioia, 1984; Brown et al., 1984; Eckstein et al., 1994) employed elastic contact algorithms, such as those implemented in the FEAP (Taylor and Sackman, 1980) and MARC finite element (FE) codes. Some authors also developed their own custom contact formulations for the sole purpose of performing diarthrodial joint contact analyses, such as Heegaard et al. (1995). These earlier investigations similarly employed nearly incompressible isotropic elastic models of cartilage.

The earliest FE models of joint contact that employed porous media formulations can be traced back to the custom mixture formulation of Schreppers et al. (1991) and the application of the ABAQUS poroelastic contact algorithm to cartilage analyses (Van der Voet et al., 1993). The poroelastic contact algorithm of the ABAQUS commercial code gained significant popularity after its capabilities were demonstrated (Wu et al., 1998) and customizations for enforcing continuity of the fluid pressure and normal flux across the contact interface were clarified (Federico et al., 2004).

A contact algorithm for biphasic models of cartilage was formulated (Donzelli and Spilker, 1998) and implemented to analyze the contact of transversely isotropic curved articular layers (Donzelli et al., 1999), showing that the location of peak tissue solid matrix stresses could now be observed not only at the cartilage–bone interface but also at the cartilage surface, consistent with experimental findings of cartilage lesions. These results demonstrated that anisotropy and articular curvature both influence the stress distribution within the tissue significantly, and the former finding is consistent with loading analysis of a transversely isotropic flat cartilage layer (Garcia et al., 1998). Another custom implementation of a biphasic contact algorithm examined the combined effects of tension–compression nonlinearity and inhomogeneity of the cartilage material properties through the articular layer thickness (Krishnan et al., 2003). This study further confirmed elevated solid matrix stresses at the articular surface on account of tension–compression nonlinearity. It also showed that inhomogeneous properties enhance the magnitude of interstitial fluid pressurization at the articular surface, where it may help reduce friction (Ateshian, 2009).

Formulations of stationary and sliding biphasic contact algorithms under finite deformation have recently been reported by several investigators, either implemented in custom codes (Chen et al., 2005; Chen and Hisada, 2007), in the commercial COMSOL code (Guo et al., 2012; Guo and Spilker, 2011, 2012), or in the open-source FEBio software suite (Ateshian et al., 2010; Maas et al., 2012) (www.febio.org). All of these formulations are valid for frictionless contact and properly enforce continuity of the normal component of the mixture traction, the fluid pressure, and the normal component of the fluid flux across the contact interface. Some recent studies have presented comparisons of biphasic contact between FEBio and ABAQUS, showing agreement as long as a user-routine is added to ABAQUS to enforce continuity of the normal component of fluid flux at the contact interface (Galbusera et al., 2012; Meng et al., 2013).

In another study it was also shown that the equivalence between the instantaneous biphasic and incompressible elastic contact responses remained valid under finite deformation (Ateshian et al., 2007). This study also presented the theoretical principles under which the pressure p in an incompressible material becomes exactly equivalent to the fluid pressure p of a biphasic material in its instantaneous response to loading. This equivalence only holds true for specific choices of constitutive relations for the solid.

A contact algorithm for triphasic models of cartilage has also been formulated recently and implemented in a custom code (Chen et al., 2009), which additionally enforces continuity of the normal component of the monovalent counter-ion fluxes as well as their electrochemical potential. A similar contact algorithm was recently

implemented in FEBio for a biphasic mixture including a neutral solute (Ateshian et al., 2012), and subsequently extended to multiphasic mixtures with charged solid matrix and any number of neutral or charged solutes (Ateshian et al., 2013).

5. Applications to three dimensional joint contact mechanics

The availability of computational algorithms for joint contact mechanics provides the opportunity to relax assumptions such as infinitesimal deformations, linear material behavior and idealized geometry. Since 3D analyses almost always make use of the FE method for spatial discretization and solution of the equations of motion, this section assumes that the FE method is the target approach.

Specific results that are sought from 3D FE analysis of contact mechanics include components and quantities derived from the stress and strain tensors, and in the case of biphasic analysis, fluid flux and fluid load support. Derived quantities of interest include contact stress, percent load supported by different regions or structures across a contact interface, and invariants of the stress and strain tensors that are related to cartilage failure such as 1st principal strain and maximum shear stress (Ateshian et al., 1994; Ateshian and Wang, 1995; Broom et al., 1996; Flachsmann et al., 1995; Radin et al., 1984; Thompson et al., 1991). The latter can provide insight into the pathogenesis of OA via comparison with values which are expected to cause physical damage or metabolic change. Evaluation on both the articular surfaces and through the thickness may be important in understanding the pathogenesis of OA (Henak et al., 2013c). For example, cartilage often fails at or near the boundary with subchondral bone (Flachsmann et al., 1995; Meachim and Bentley, 1978).

The primary inputs required for 3D FE models of contact mechanics include the geometry of the articulating surfaces and other structures involved in load support or transfer across the joint (e.g., meniscus, labrum, ligaments, tendons, depending on the loading scenarios of interest), material properties for constitutive models, and boundary and loading conditions (Fig. 1). Acquisition and processing of geometry is especially challenging for 3D models. For modeling joint contact mechanics in vivo, the geometry is primarily obtained via volumetric computed tomography (CT) or magnetic resonance (MR) imaging. The cartilage–cartilage and cartilage–bone interfaces must be clearly visible over the entire articular surfaces to allow reconstruction of articular cartilage geometry (Anderson et al., 2010a). This goal is challenging because articulating joints are often surrounded by thick musculature, ligaments and tendons. Articular surfaces of congruent joints such as the hip are often in close contact even in the absence of external loading or body weight. In some cases, this issue can be addressed by the intra-articular injection of a contrast agent, which serves both to separate the joint surfaces and to provide contrast between the articular layers.

The primary benefits of CT are excellent visualization of bone and cartilage and short scan times, which help to ensure minimal motion artifact. High-resolution CT provides excellent delineation of bone, and can be used to image opposing layers of cartilage with contrast enhancement (Allen et al., 2010; Eckstein et al., 2005; El-Khoury et al., 2004; Wyler et al., 2009). The primary drawbacks to CT arthrography (CTA) are exposure to ionizing radiation and the invasive nature of the injection of contrast agent. In our studies of patient-specific contact mechanics in the hip using CTA [185, 186], 15–25 ml of diluted contrast agent is injected into the joint, followed directly by CT image acquisition while the hip is under traction (Henak et al., 2013e, 2014). Additional considerations for volumetric CT image acquisition include position and orientation of the joint in the scanner, field of view and energy/scanner settings.

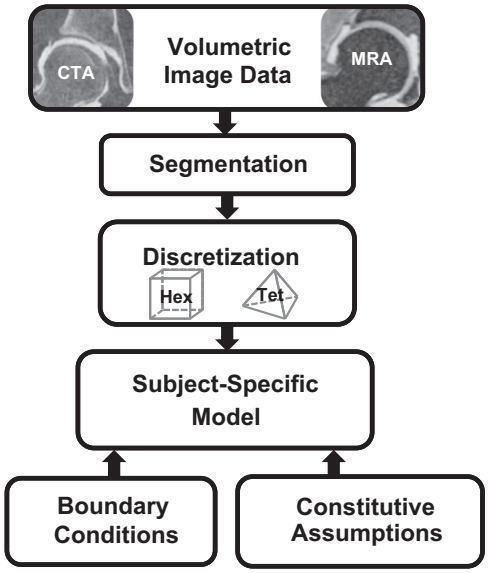

Fig. 1. High-level flowchart of methods for generating subject-specific finite element models of joint contact mechanics from in vivo medical image data. The source for geometry is typically obtained from CT arthrography (CTA) or MR arthrography (MRA) data. The injected contrast separates the articular layers and highlights the cartilage surfaces (Anderson et al., 2008b). Because of the complex boundaries that are produced by the contrast agent, manual segmentation is often necessary to identify the cartilage surface and the cartilage–bone boundaries. Typical finite element discretization strategies involve the use of hexahedral and/or tetrahedral elements. Discretization of the articular layers is especially difficult since the cartilage is thin and multiple elements are needed through the thickness to resolve gradients in stress and strain (Henak et al., 2013c). When combined with generic or patient-specific boundary and loading conditions, and appropriate material data, these inputs provide the basis for finite element analysis of subject-specific joint contact mechanics (Harris et al., 2012; Henak et al., 2014; Henak et al., 2013d).

Please see our recent review article for more details on the use of CT for FE model creation (Henak et al., 2013b).

MR arthrography (MRA) is an attractive alternative to CTA since there is no radiation exposure. However, clinical protocols for imaging articular cartilage often use 2D acquisitions that are not SNR-efficient and produce relatively thick slices that suffer from non-uniform slice profiles and staircase artifact. 3D acquisitions require longer scan times, but for joints such as the knee that have minimal overlying soft tissue, the scan times are still reasonable. The most important factors to consider when acquiring MR image data to create 3D models are signal to noise ratio (SNR), spatial resolution, field strength, scan protocol, use of coils and orientation of scan plane (Gold et al., 2009, 2012; Potter et al., 2009; Potter and Schachar, 2010; Recht et al., 2005; Shapiro et al., 2012). High spatial resolution and adequate SNR must be balanced to obtain high-quality MR images (Recht et al., 2005). Unlike CT, MR can acquire native scans in all three anatomical planes.

After volumetric image data are available, segmentation and discretization are the next technical hurdles on the path to mesh generation (Fig. 1). Segmentation is the process of identifying the boundaries of specific tissues in volumetric image data, and discretization is the process of mesh generation from the segmented image data. The most effective approach to segmentation varies between datasets, but all function primarily using methods such as thresholding, histogram based segmentation and manual segmentation. The 3D geometry can be reconstructed from the 2D segmentation masks via several methods, and the result is often a triangulated surface (Boissonnat, 1988). Decimation and smoothing can be applied to refine the surface (Schneider et al., 2012; Taubin et al., 1996). Accuracy of the segmented surfaces is an important consideration in both automatic and manual segmentation (Allen et al.,

2010; Cohen et al., 1999; Li et al., 2008b; Stammberger et al., 1999) as it will affect the accuracy of model predictions.

6. Subject- and patient-specific analysis

When the ability to perform three-dimensional (3D) FE contact analysis is available, subject-specific geometry can be analyzed. This provides the opportunity to examine normal populations of individuals and populations with specific injuries or other pathologies. Ultimately, patient-specific modeling offers the potential for use in surgical planning and for large scale studies of treatment efficacy. Such approaches have already seen some application in the hip, knee and ankle (Adouni and Shirazi-Adl, 2014; Anderson et al., 2010b; Fitzpatrick et al., 2012; Henak et al., 2014; Henak et al., 2013a; Li et al., 2008a; Wang et al., 2014). The following section focuses on our own research related to patient-specific modeling of the hip.

Over the past 13 years, we developed and validated a patient-specific FE (FE) analysis pipeline to examine cartilage mechanics in the hip, and we studied 84 normal volunteers and patients with acetabular dysplasia and acetabular retroversion (Anderson et al., 2008a, 2010a, 2008b, 2005; Harris et al., 2012; Henak et al., 2014, 2013b, 2013c, 2013d, 2011). The most common type of dysplasia ("traditional dysplasia") is characterized by a shallow acetabulum and lack of coverage of the femoral head (Cooperman et al., 1983). The benefit of patient-specific FE modeling for this population becomes clear when one considers that it would be nearly impossible to assemble a population of cadaver tissue that exhibits a pathology such as acetabular dysplasia. Our findings demonstrate that increased labral loading, rather than higher contact stresses on acetabular or femoral cartilage, is the primary distinguishing characteristic of hips with traditional dysplasia () (Fig. 2). Indeed, congruency and contact area are not substantially different in the primary load-bearing regions, challenging the hypothesis that chronic contact stress overload due to reduced congruency is the cause of early onset OA in dysplastic hips. Further, our results support clinical observations of OA progression for relatively young patients with acetabular dysplasia versus older patients. In patients with traditional dysplasia and early OA, labral tears and peripheral damage to the acetabular cartilage and delamination are the most common findings (Akiyama et al., 2013; Dorrell and Catterall, 1986; Fujii et al., 2009; Hartig-Andreasen et al., 2013; McCarthy et al., 2003, 2001a, 2001b; Tamura et al., 2012; Thomas et al., 2013). In contrast, older patients with early OA typically exhibit progressive joint space narrowing (Conrozier et al., 1998; Franklin et al., 2011; Goker et al., 2000).

Subsequently, we used a population of validated FE models of normal human hips to resolve transchondral predictions of cartilage tensile strain and shear stress (Henak et al., 2013c) (Fig. 3). We specifically focused on variation through the thickness of the cartilage between the articular surface and the osteochondral interface during simulated activities of daily living. Using highly refined meshes through the cartilage thickness for five specimen-specific models, we were able to predict the expected elevation in maximum shear stress at the cartilage–bone boundary on the femoral side (Fig. 3C), and that the highest shear stresses on both acetabular and femoral sides occurred at the cartilage–bone boundary (Fig. 3B). With further validation of cartilage failure criteria, the results of this study demonstrate the potential for FE modeling of joint contact mechanics to predict cartilage failure on a patient-specific basis.

7. Challenges and future directions

The material behavior of articular cartilage has been studied in detail for decades, and we understand the effects of anisotropy, tension–compression nonlinearity, inhomogeneity and flow-induced viscoelasticity on the predicted stress response of articular cartilage for many idealized situations. Yet, in terms of 3D modeling, we still lack information on which assumptions are appropriate and reasonable for simulating different types of loading scenarios. Additionally, there is a dearth of experimental test data for even normal human articular cartilage from joints of clinical interest such as the hip and knee that is suitable for populating anisotropic, inhomogeneous 3D constitutive models. Most of the available data have been obtained for bovine articular cartilage. Similarly, minimal data are available for normal meniscus, hip labrum, and other important load bearing structures that must be represented in 3D models. Further research is needed in all of these areas.

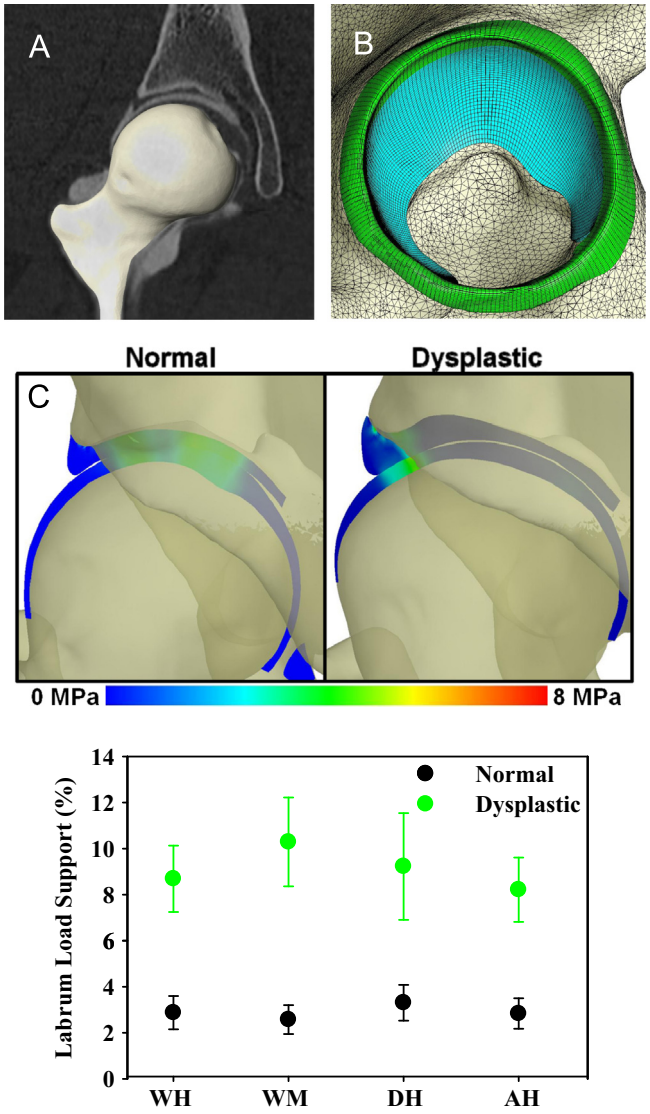

Fig. 2. Patient-specific FE analysis of hip contact mechanics reveals differences in loading of the labrum between normal and dysplastic hips (Henak et al., 2014). (A) Manual segmentation of osteochondral boundary from volumetric CT arthrography data allows surface reconstruction (beige). (B) FE mesh of articular layers, labrum, pelvis and proximal femur. (C) Coronal cross-sectional images of pressure in representative normal (left) and dysplastic (right) hips, with the bones rendered as transparent. Lateral loading in the dysplastic hip results in higher contact stress in the acetabular labrum, and thus larger loads. (D) Percent load supported by the labrum during simulated activities of walking heelstrike (WH), walking midstance (WM), descending stairs heelstrike (DH) and ascending stairs heelstrike (AH). Load supported by the labrum was significantly larger for dysplastic hips than normal hips during all loading scenarios. Error bars indicate upper confidence bounds (at 95%). *Indicates $p \leq 0.05$ in comparison to normal hips during the same loading scenario ($n=10$ in each group).

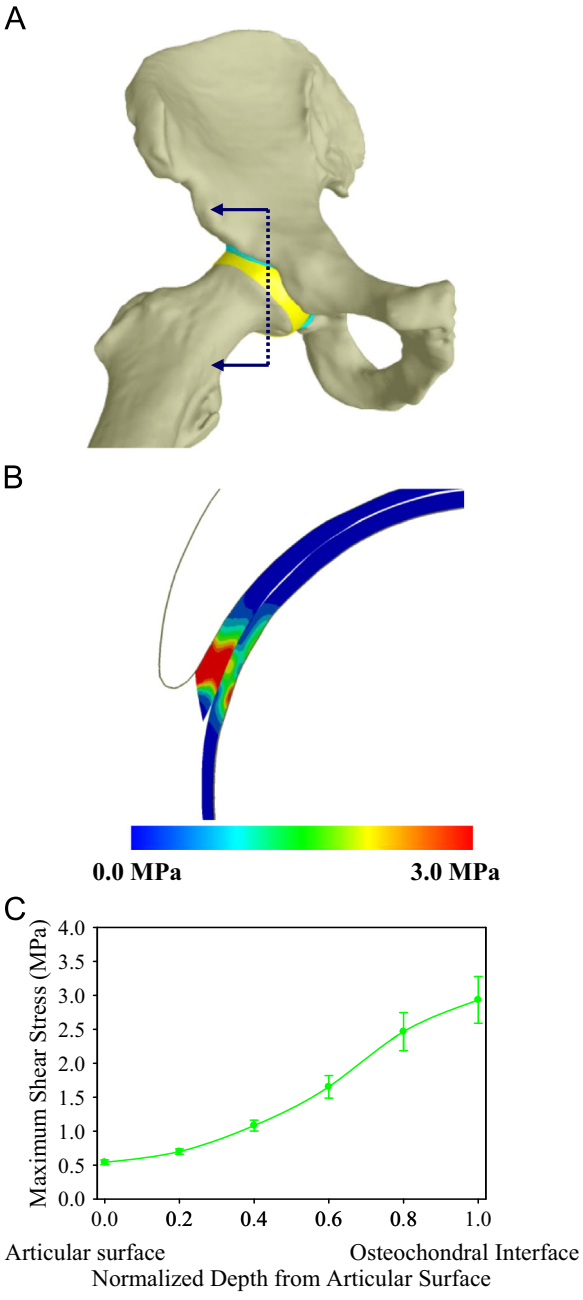

Fig. 3. Transchondral stress and strain predictions offer the potential ability to predict cartilage overload and failure due to specific pathomorphologies such as dysplasia and femoroacetabular impingement (Henak et al., 2013c). (A) Finite element model for one of the five specimens, showing the cutting plane used to sample transchondral results. (B) Fringe plot of maximum shear stress through the thickness of the acetabular and femoral cartilage layers for the specimen shown in panel A. Peak values of maximum shear stress occurred at the osteochondral interfaces. (C) Average of the maximum shear stress through the thickness of the femoral articular cartilage during ascending stairs heelstrike across all samples. Error bars = standard deviation.

Despite the success with CTA, the process of generating a FE model from CTA image data is painfully slow, taking over 100 h for segmentation and mesh generation. Better methods are needed for segmenting the articular cartilage layers from this image modality as well as from MRA to automate the process. With an order of magnitude improvement in time for model creation, patient specific modeling of articular contact mechanics would become a feasible addition to clinical diagnosis and treatment planning. Additionally, improved MRI methods are needed for imaging deep joints such as the hip. Current clinical MRI protocols do not address the needs of 3D model reconstruction and do not provide sufficient signal-to-noise ratio when imaging deep joints. Additional time savings can come from improved methods for mesh generation, and techniques such as statistical shape modeling may help to reuse existing models by mapping them to new patients.

Finally, many questions remain regarding the need for subject-specific boundary and loading conditions, and subject-specific material properties. In our own studies (Anderson et al., 2008a, 2010a; Harris et al., 2012; Henak et al., 2014), most of our simulations to date have utilized generic, population average data for kinetics. It is likely that for some populations, subject-specific kinematics and kinetics will be necessary to obtain reasonable predictions of stress and strain during joint contact analysis. Similar questions apply for material properties, especially for populations expected to have far-from-average articular cartilage such as advanced osteoarthritis.

In the future, databases consisting of model geometry, mechanical results and other relevant data could provide the basis for quick classification of patients. By indexing multiple measures from a patient into such a database, decisions regarding diagnosis and treatment planning may be able to be made without performing any further computational contact analysis.

Acknowledgments

Research was supported by the National Institute of Arthritis and Musculoskeletal and Skin Diseases and the National Institute of General Medical Sciences of the National Institutes of Health under Awards R01AR043628, R01AR053344, and R01GM083925. Content is solely the responsibility of the authors and does not necessarily represent official views of the National Institutes of Health. Dr. Weiss thanks the faculty, students and staff who contributed to research on hip contact mechanics, including Andrew E. Anderson, Benjamin J. Ellis, Christopher L. Peters, Corinne Henak, Michael Harris and Steve A Maas.

References

Adouni, M., Shirazi-Adl, A., 2014. Evaluation of knee joint muscle forces and tissue stresses-strains during gait in severe OA versus normal subjects. J. Orthop. Res.: Off. Publ. Orth. Res. Soc. 32, 69–78.

Akiyama, K., Sakai, T., Koyanagi, J., Yoshikawa, H., Sugamoto, K., 2013. In vivo hip joint contact distribution and bony impingement in normal and dysplastic human hips. J. Orthop. Res.: Off. Publ. Orth. Res. Soc..

Allen, B.C., Peters, C.L., Brown, N.A., Anderson, A.E., 2010. Acetabular cartilage thickness: accuracy of three-dimensional reconstructions from multidetector CT arthrograms in a cadaver study. Radiology 255, 544–552 (PMCID: 2858813).

Anderson, A.E., Ellis, B.J., Maas, S.A., Peters, C.L., Weiss, J.A., 2008a. Validation of finite element predictions of cartilage contact pressure in the human hip joint. J. Biomech. Eng. 130, 051008 (PMCID: 2840996).

Anderson, A.E., Ellis, B.J., Maas, S.A., Weiss, J.A., 2010a. Effects of idealized joint geometry on finite element predictions of cartilage contact stresses in the hip. J. Biomech. 43, 1351–1357 (PMCID: 2857573).

Anderson, A.E., Ellis, B.J., Peters, C.L., Weiss, J.A., 2008b. Cartilage thickness: factors influencing multidetector CT measurements in a phantom study. Radiology 246, 133–141 (PMCID: 2881220).

Anderson, A.E., Peters, C.L., Tuttle, B.D., Weiss, J.A., 2005. Subject-specific finite element model of the pelvis: development, validation and sensitivity studies. J. Biomech. Eng. 127, 364–373.

Anderson, D.D., Iyer, K.S., Segal, N.A., Lynch, J.A., Brown, T.D., 2010b. Implementation of discrete element analysis for subject-specific, population-wide investigations of habitual contact stress exposure. J. Appl. Biomech. 26, 215–223 (PMCID: 2905528).

Armstrong, C.G., 1986. An analysis of the stresses in a thin layer of articular cartilage in a synovial joint. Eng. Med. 15, 55–61.

Armstrong, C.G., Lai, W.M., Mow, V.C., 1984. An analysis of the unconfined compression of articular cartilage. J. Biomech. Eng. 106, 165–173.

Armstrong, C.G., Mow, V.C., 1982. Variations in the intrinsic mechanical properties of human articular cartilage with age, degeneration, and water content. J. Bone Joint Surg. Am. 64, 88–94.

Ateshian, G.A., 2009. The role of interstitial fluid pressurization in articular cartilage lubrication. J. Biomech. 42, 1163–1176 (PMCID: PMC2758165).

Ateshian, G.A., Ellis, B.J., Weiss, J.A., 2007. Equivalence between short-time biphasic and incompressible elastic material responses. J. Biomech. Eng. 129, 405–412 (PMCID: 3312381).
Ateshian, G.A., Lai, W.M., Zhu, W.B., Mow, V.C., 1994. An asymptotic solution for the contact of two biphasic cartilage layers. J. Biomech. 27, 1347–1360.
Ateshian, G.A., Maas, S., Weiss, J.A., 2010. Finite element algorithm for frictionless contact of porous permeable media under finite deformation and sliding. J. Biomech. Eng. 132, 061006 (PMCID: 2953263).
Ateshian, G.A., Maas, S., Weiss, J.A., 2012. Solute transport across a contact interface in deformable porous media. J. Biomech. 45, 1023–1027 (PMCID: 3351088).
Ateshian, G.A., Maas, S., Weiss, J.A., 2013. Multiphasic finite element framework for modeling hydrated mixtures with multiple neutral and charged solutes. J. Biomech. Eng. 135, 111001 (PMCID: 3792408).
Ateshian, G.A., Rajan, V., Chahine, N.O., Canal, C.E., Hung, C.T., 2009. Modeling the matrix of articular cartilage using a continuous fiber angular distribution predicts many observed phenomena. J. Biomech. Eng. 131, 061003 (PMCID: 2842192).
Ateshian, G.A., Wang, H., 1995. A theoretical solution for the frictionless rolling contact of cylindrical biphasic articular cartilage layers. J. Biomech. 28, 1341–1355.
Ateshian, G.A., Warden, W.H., Kim, J.J., Grelsamer, R.P., Mow, V.C., 1997. Finite deformation biphasic material properties of bovine articular cartilage from confined compression experiments. J. Biomech. 30, 1157–1164.
Basser, P.J., Schneiderman, R., Bank, R.A., Wachtel, E., Maroudas, A., 1998. Mechanical properties of the collagen network in human articular cartilage as measured by osmotic stress technique. Arch. Biochem. Biophys. 351, 207–219.
Boissonnat, J.-D., 1988. Shape reconstruction from planar cross sections. Comput. Vis. Graph. Image Process. 44, 1–29.
Bowen, R.M., 1976. Theory of Mixtures. Academic Press, New York.
Bowen, R.M., 1980. Incompressible porous media models by use of the theory of mixtures. Int. J. Eng. Sci. 18, 1129–1148.
Broom, N.D., Oloyede, A., Flachsmann, R., Hows, M., 1996. Dynamic fracture characteristics of the osteochondral junction undergoing shear deformation. Med. Eng. Phys. 18, 396–404.
Brown, T.D., DiGioia 3rd, A.M., 1984. A contact-coupled finite element analysis of the natural adult hip. J. Biomech. 17, 437–448.
Brown, T.D., Radin, E.L., Martin, R.B., Burr, D.B., 1984. Finite element studies of some juxtarticular stress changes due to localized subchondral stiffening. J. Biomech. 17, 11–24.
Brown, T.D., Singerman, R.J., 1986. Experimental determination of the linear biphasic constitutive coefficients of human fetal proximal femoral chondroepiphysis. J. Biomech. 19, 597–605.
Chen, X., Chen, Y., Hisada, T., 2005. Development of a finite element procedure of contact analysis for articular cartilage with large deformation based on the biphasic theory. JSME Int. J. Ser. C (Mech. Syst. Mach. Elem. Manuf.) 48, 537–546.
Chen, X., Hisada, T., 2007. Development of a finite element contact analysis algorithm to pass the patch test. JSME Int. J. Ser. A: Solid Mech. Mater. Eng. 49, 483–491.
Chen, X., Sunagawa, K., Hisada, T., 2009. Development of a finite element contact analysis algorithm for charged-hydrated soft tissues with large sliding. Int. J. Numer. Methods Eng. 78, 483–504.
Cohen, B., Lai, W.M., Mow, V.C., 1998. A transversely isotropic biphasic model for unconfined compression of growth plate and chondroepiphysis. J. Biomech. Eng. 120, 491–496.
Cohen, Z.A., McCarthy, D.M., Kwak, S.D., Legrand, P., Fogarasi, F., Ciaccio, E.J., Ateshian, G.A., 1999. Knee cartilage topography, thickness, and contact areas from MRI: in-vitro calibration and in-vivo measurements. Osteoarthr. Cartil. 7, 95–109.
Conrozier, T., Jousseaume, C.A., Mathieu, P., Tron, A.M., Caton, J., Bejui, J., Vignon, E., 1998. Quantitative measurement of joint space narrowing progression in hip osteoarthritis: a longitudinal retrospective study of patients treated by total hip arthroplasty. Br. J. Rheumatol. 37, 961–968.
Cooperman, D.R., Wallensten, R., Stulberg, S.D., 1983. Acetabular dysplasia in the adult. Clin. Orthop. Relat. Res., 79–85.
DiSilvestro, M.R., Zhu, Q., Suh, J.K., 2001a. Biphasic poroviscoelastic simulation of the unconfined compression of articular cartilage: II—Effect of variable strain rates. J. Biomech. Eng. 123, 198–200.
DiSilvestro, M.R., Zhu, Q., Wong, M., Jurvelin, J.S., Suh, J.K., 2001b. Biphasic poroviscoelastic simulation of the unconfined compression of articular cartilage: I—Simultaneous prediction of reaction force and lateral displacement. J. Biomech. Eng. 123, 191–197.
Donzelli, P.S., Spilker, R.L., 1998. A contact finite element formulation for biological soft hydrated tissues. Comput. Methods Appl. Mech. Eng. 153, 63–79.
Donzelli, P.S., Spilker, R.L., Ateshian, G.A., Mow, V.C., 1999. Contact analysis of biphasic transversely isotropic cartilage layers and correlations with tissue failure. J. Biomech. 32, 1037–1047.
Dorrell, J.H., Catterall, A., 1986. The torn acetabular labrum. J. Bone Joint Surg. Br. Vol. 68, 400–403.
Eberhardt, A.W., Keer, L.M., Lewis, J.L., Vithoontien, V., 1990. An analytical model of joint contact. J. Biomech. Eng. 112, 407–413.
Eberhardt, A.W., Lewis, J.L., Keer, L.M., 1991a. Contact of layered elastic spheres as a model of joint contact: effect of tangential load and friction. J. Biomech. Eng. 113, 107–108.
Eberhardt, A.W., Lewis, J.L., Keer, L.M., 1991b. Normal contact of elastic spheres with two elastic layers as a model of joint articulation. J. Biomech. Eng. 113, 410–417.
Eckstein, F., Charles, H.C., Buck, R.J., Kraus, V.B., Remmers, A.E., Hudelmaier, M., Wirth, W., Evelhoch, J.L., 2005. Accuracy and precision of quantitative assessment of cartilage morphology by magnetic resonance imaging at 3.0T. Arthritis Rheum. 52, 3132–3136.
Eckstein, F., Merz, B., Schmid, P., Putz, R., 1994. The influence of geometry on the stress distribution in joints—a finite element analysis. Anat. Embryol. 189, 545–552.
El-Khoury, G.Y., Alliman, K.J., Lundberg, H.J., Rudert, M.J., Brown, T.D., Saltzman, C.L., 2004. Cartilage thickness in cadaveric ankles: measurement with double-contrast multi-detector row CT arthrography versus MR imaging. Radiology 233, 768–773.
Elmore, S.M., Sokoloff, L., Norris, G., Carmeci, P., 1963. Nature of "imperfect" elasticity of articular cartilage. J. Appl. Physiol. 18, 393–396.
Federico, S., La Rosa, G., Herzog, W., Wu, J.Z., 2004. Effect of fluid boundary conditions on joint contact mechanics and applications to the modeling of osteoarthritic joints. J. Biomech. Eng. 126, 220–225.
Fitzpatrick, C.K., Clary, C.W., Rullkoetter, P.J., 2012. The role of patient, surgical, and implant design variation in total knee replacement performance. J. Biomech. 45, 2092–2102.
Flachsmann, E.R., Broom, N.D., Oloyede, A., 1995. A biomechanical investigation of unconstrained shear failure of the osteochondral region under impact loading. Clin. Biomech. 10, 156–165.
Franklin, J., Ingvarsson, T., Englund, M., Ingimarsson, O., Robertsson, O., Lohmander, L.S., 2011. Natural history of radiographic hip osteoarthritis: a retrospective cohort study with 11–28 years of followup. Arthritis Care Res. 63, 689–695.
Freeman, M.A.R., 1979. Adult Articular Cartilage. Pitman Medical, Tunbridge Wells, Eng..
Fujii, M., Nakashima, Y., Jingushi, S., Yamamoto, T., Noguchi, Y., Suenaga, E., Iwamoto, Y., 2009. Intraarticular findings in symptomatic developmental dysplasia of the hip. J. Pediatr. Orthop. 29, 9–13.
Galbusera, F., Bashkuev, M., Wilke, H.J., Shirazi-Adl, A., Schmidt, H., 2012. Comparison of various contact algorithms for poroelastic tissues. Comput. Methods Biomech. Biomed. Eng..
Garcia, J.J., Altiero, N.J., Haut, R.C., 1998. An approach for the stress analysis of transversely isotropic biphasic cartilage under impact load. J. Biomech. Eng. 120, 608–613.
Goker, B., Doughan, A.M., Schnitzer, T.J., Block, J.A., 2000. Quantification of progressive joint space narrowing in osteoarthritis of the hip: longitudinal analysis of the contralateral hip after total hip arthroplasty. Arthritis Rheumatol. 43, 988–994.
Gold, G.E., Chen, C.A., Koo, S., Hargreaves, B.A., Bangerter, N.K., 2009. Recent advances in MRI of articular cartilage. Am. J. Roentgenol. 193, 628–638 (PMCID: 2879429).
Gold, S.L., Burge, A.J., Potter, H.G., 2012. MRI of hip cartilage: joint morphology, structure, and composition. Clin. Orthop. Relat. Res..
Gu, W.Y., Lai, W.M., Mow, V.C., 1998. A mixture theory for charged-hydrated soft tissues containing multi-electrolytes: passive transport and swelling behaviors. J. Biomech. Eng. 120, 169–180.
Guo, H., Nickel, J.C., Iwasaki, L.R., Spilker, R.L., 2012. An augmented Lagrangian method for sliding contact of soft tissue. J. Biomech. Eng. 134, 084503 (PMCID: 3488455).
Guo, H., Spilker, R.L., 2011. Biphasic finite element modeling of hydrated soft tissue contact using an augmented Lagrangian method. J. Biomech. Eng. 133, 111001 (PMCID: 3313488).
Guo, H., Spilker, R.L., 2012. An augmented Lagrangian finite element formulation for 3D contact of biphasic tissues. Comput. Methods Biomech. Biomed. Eng. (PMCID: 3587284).
Harris, M.D., Anderson, A.E., Henak, C.R., Ellis, B.J., Peters, C.L., Weiss, J.A., 2012. Finite element prediction of cartilage contact stresses in normal human hips. J. Orthop. Res.: Off. Publ. Orthop. Res. Soc. 30, 1133–1139 (PMCID: 3348968).
Hartig-Andreasen, C., Soballe, K., Troelsen, A., 2013. The role of the acetabular labrum in hip dysplasia. A literature overview. Acta Orthop. 84, 60–64 (PMCID: 3584604).
Hayes, W.C., Bodine, A.J., 1978. Flow-independent viscoelastic properties of articular cartilage matrix. J. Biomech. 11, 407–419.
Hayes, W.C., Keer, L.M., Herrmann, G., Mockros, L.F., 1972. A mathematical analysis for indentation tests of articular cartilage. J. Biomech. 5, 541–551.
Hayes, W.C., Mockros, L.F., 1971. Viscoelastic properties of human articular cartilage. J. Appl. Physiol. 31, 562–568.
Heegaard, J., Leyvraz, P.F., Curnier, A., Rakotomanana, L., Huiskes, R., 1995. The biomechanics of the human patella during passive knee flexion. J. Biomech. 28, 1265–1279.
Henak, C.R., Abraham, C.L., Anderson, A.E., Maas, S.A., Ellis, B.J., Peters, C.L., Weiss, J.A., 2014. Patient-specific analysis of cartilage and labrum mechanics in human hips with acetabular dysplasia. Osteoarthr. Cartil. 22, 210–217.
Henak, C.R., Anderson, A.E., Weiss, J.A., 2013a. Subject-specific analysis of joint contact mechanics: application to the study of osteoarthritis and surgical planning. J. Biomech. Eng. 135, 021003 (PMCID: 3705883).
Henak, C.R., Anderson, A.E., Weiss, J.A., 2013b. Subject-specific analysis of joint contact mechanics: application to the study of osteoarthritis and surgical planning. J. Biomech. Eng. 135, 021003 (PMCID: 3705883).
Henak, C.R., Ateshian, G.A., Weiss, J.A., 2013c. Finite element prediction of transchondral stress and strain in the human hip. J. Biomech. Engineering.
Henak, C.R., Carruth, E.D., Anderson, A.E., Harris, M.D., Ellis, B.J., Peters, C.L., Weiss, J.A., 2013d. Finite element predictions of cartilage contact mechanics in hips with retroverted acetabula. Osteoarthr. Cartil. 21, 1522–1529 (PMCID: 3779536).

Henak, C.R., Carruth, E., Anderson, A.E., Harris, M.D., Ellis, B.J., Peters, C.L., Weiss, J.A., 2013e. Finite element predictions of cartilage contact mechanics in hips with retroverted acetabula. Osteoarthr. Cartil. 21 (10), 1522–1529. http://dx.doi.org/10.1016/j.joca.2013.06.008.

Henak, C.R., Ellis, B.J., Harris, M.D., Anderson, A.E., Peters, C.L., Weiss, J.A., 2011. Role of the acetabular labrum in load support across the hip joint. J. Biomech, 44, 2201–2206 (PMCID: 3225073).

Holmes, M.H., Lai, W.M., Mow, V.C., 1985. Singular perturbation analysis of the nonlinear, flow-dependent compressive stress relaxation behavior of articular cartilage. J. Biomech. Eng. 107, 206–218.

Huang, C.Y., Mow, V.C., Ateshian, G.A., 2001. The role of flow-independent viscoelasticity in the biphasic tensile and compressive responses of articular cartilage. J. Biomech. Eng. 123, 410–417.

Huang, C.Y., Soltz, M.A., Kopacz, M., Mow, V.C., Ateshian, G.A., 2003. Experimental verification of the roles of intrinsic matrix viscoelasticity and tension-compression nonlinearity in the biphasic response of cartilage. J. Biomech. Eng. 125, 84–93.

Huang, C.Y., Stankiewicz, A., Ateshian, G.A., Mow, V.C., 2005. Anisotropy, inhomogeneity, and tension-compression nonlinearity of human glenohumeral cartilage in finite deformation. J. Biomech. 38, 799–809.

Huyghe, J.M., Janssen, J.D., 1997. Quadriphasic mechanics of swelling incompressible porous media. Int. J. Eng. Sci. 35, 793–802.

Johnson, K.L., 1985. Contact Mechanics. Cambridge University Press, Cambridge [Cambridgeshire], New York.

Kelkar, R., Ateshian, G.A., 1999. Contact creep of biphasic cartilage layers. Trans ASME J. Appl. Mech. 66, 137–145.

Kempson, G.E., Freeman, M.A., Swanson, S.A., 1968. Tensile properties of articular cartilage. Nature 220, 1127–1128.

Krishnan, R., Park, S., Eckstein, F., Ateshian, G.A., 2003. Inhomogeneous cartilage properties enhance superficial interstitial fluid support and frictional properties, but do not provide a homogeneous state of stress. J. Biomech. Eng. 125, 569–577.

Lai, W.M., Hou, J.S., Mow, V.C., 1991. A triphasic theory for the swelling and deformation behaviors of articular cartilage. J. Biomech. Eng. 113, 245–258.

Li, W., Anderson, D.D., Goldsworthy, J.K., Marsh, J.L., Brown, T.D., 2008a. Patient-specific finite element analysis of chronic contact stress exposure after intraarticular fracture of the tibial plafond. J. Orthop. Res.: Off. Publ. Orthop. Res. Soc. 26, 1039–1045 (PMCID: 2562934).

Li, W., Anderson, D.D., Goldsworthy, J.K., Marsh, J.L., Brown, T.D., 2008b. Patient-specific finite element analysis of chronic contact stress exposure after intraarticular fracture of the tibial plafond. J. Orthop. Res.: Off. Publ. Orthop. Res. Soc. 26, 1039–1045.

Maas, S.A., Ellis, B.J., Ateshian, G.A., Weiss, J.A., 2012. FEBio: finite elements for biomechanics. J. Biomech. Eng. 134, 011005.

Maroudas, A., 1968. Physicochemical properties of cartilage in the light of ion exchange theory. Biophys. J. 8, 575–595.

Mauck, R.L., Hung, C.T., Ateshian, G.A., 2003. Modeling of neutral solute transport in a dynamically loaded porous permeable gel: implications for articular cartilage biosynthesis and tissue engineering. J. Biomech. Eng. 125, 602–614 (PMCID: 2854001).

McCarthy, J., Noble, P., Aluisio, F.V., Schuck, M., Wright, J., Lee, J.A., 2003. Anatomy, pathologic features, and treatment of acetabular labral tears. Clin. Orthop. Relat. Res., 38–47.

McCarthy, J.C., Noble, P.C., Schuck, M.R., Wright, J., Lee, J., 2001a. The Otto E. Aufranc Award: the role of labral lesions to development of early degenerative hip disease. Clin. Orthop. Relat. Res., 25–37.

McCarthy, J.C., Noble, P.C., Schuck, M.R., Wright, J., Lee, J., 2001b. The watershed labral lesion: its relationship to early arthritis of the hip. J. Arthroplast. 16, 81–87.

Meachim, G., Bentley, G., 1978. Horizontal splitting in patellar articular cartilage. Arthritis Rheumatol. 21, 669–674.

Meng, Q., Jin, Z., Fisher, J., Wilcox, R., 2013. Comparison between FEBio and Abaqus for biphasic contact problems. Proc. Inst. Mech. Eng. H 227, 1009–1019 (PMCID: 3834732).

Mow, V.C., Huiskes, R., 2005. Basic Orthopaedic Biomechanics & Mechano-biology. Lippincott Williams & Wilkins, Philadelphia, PA.

Mow, V.C., Kuei, S.C., Lai, W.M., Armstrong, C.G., 1980. Biphasic creep and stress relaxation of articular cartilage in compression? Theory and experiments. J. Biomech. Eng. 102, 73–84.

Park, S., Ateshian, G.A., 2006. Dynamic response of immature bovine articular cartilage in tension and compression, and nonlinear viscoelastic modeling of the tensile response. J. Biomech. Eng. 128, 623–630 (PMCID: 2842191).

Park, S., Hung, C.T., Ateshian, G.A., 2004. Mechanical response of bovine articular cartilage under dynamic unconfined compression loading at physiological stress levels. Osteoarthr. Cartil. 12, 65–73.

Park, S., Krishnan, R., Nicoll, S.B., Ateshian, G.A., 2003. Cartilage interstitial fluid load support in unconfined compression. J. Biomech. 36, 1785–1796.

Potter, H.G., Black, B.R., le, R., Chong, 2009. New techniques in articular cartilage imaging. Clin. Sports Med. 28, 77–94.

Potter, H.G., Schachar, J., 2010. High resolution noncontrast MRI of the hip. J. Magn. Reson. Imaging 31, 268–278.

Radin, E.L., Martin, R.B., Burr, D.B., Caterson, B., Boyd, R.D., Goodwin, C., 1984. Effects of mechanical loading on the tissues of the rabbit knee. J. Orthop. Res.: Off. Publ. Orthop. Res. Soc. 2, 221–234.

Recht, M.P., Goodwin, D.W., Winalski, C.S., White, L.M., 2005. MRI of articular cartilage: revisiting current status and future directions. Am. J. Roentgenol. 185, 899–914.

Schneider, E., Nevitt, M., McCulloch, C., Cicuttini, F.M., Duryea, J., Eckstein, F., Tamez-Pena, J., 2012. Equivalence and precision of knee cartilage morphometry between different segmentation teams, cartilage regions, and MR acquisitions. Osteoarthr. Cartil. 20, 869–879 (PMCID: 3391588).

Schreppers, G.J., Sauren, A.A., Huson, A., 1991. A model of force transmission in the tibio-femoral contact incorporating fluid and mixtures. Proc. Inst. Mech. Eng. H 205, 233–241.

Shapiro, L., Harish, M., Hargreaves, B., Staroswiecki, E., Gold, G., 2012. Advances in musculoskeletal MRI: technical considerations. J. Magn. Reson. Imaging 36, 775–787 (PMCID: 3448292).

Soltz, M.A., Ateshian, G.A., 1998. Experimental verification and theoretical prediction of cartilage interstitial fluid pressurization at an impermeable contact interface in confined compression. J. Biomech. 31, 927–934.

Soltz, M.A., Ateshian, G.A., 2000a. A conewise linear elasticity mixture model for the analysis of tension-compression nonlinearity in articular cartilage. J. Biomech. Eng. 122, 576–586 (PMCID: 2854000).

Soltz, M.A., Ateshian, G.A., 2000b. Interstitial fluid pressurization during confined compression cyclical loading of articular cartilage. Ann. Biomed. Eng. 28, 150–159.

Soulhat, J., Buschmann, M.D., Shirazi-Adl, A., 1999. A fibril-network-reinforced biphasic model of cartilage in unconfined compression. J. Biomech. Eng. 121, 340–347.

Stammberger, T., Eckstein, F., Michaelis, M., Englmeier, K.H., Reiser, M., 1999. Interobserver reproducibility of quantitative cartilage measurements: comparison of B-spline snakes and manual segmentation. Magn. Reson. Imaging 17, 1033–1042.

Tamura, S., Nishii, T., Shiomi, T., Yamazaki, Y., Murase, K., Yoshikawa, H., Sugano, N., 2012. Three-dimensional patterns of early acetabular cartilage damage in hip dysplasia; a high-resolutional CT arthrography study. Osteoarthr. Cartil. 20, 646–652.

Taubin, G., Zhang, T., Golub, G., 1996. Optimal surface smoothing as filter design. In: Buxton, B., Cipolla R. (Eds.), Computer Vision – ECCV'96. Springer, Berlin/Heidelberg, pp. 283–292.

Taylor, R., Sackman, J., 1980. Contact-Impact Problems. Volume 1: Engineering Report and User's Manual. University of California, Berkeley National Highway Traffic Safety Administration.

Thomas, J.D., Li, Z., Agur, A.M., Robinson, P., 2013. Imaging of the acetabular labrum. Semin. Musculoskelet. Radiol. 17, 248–257.

Thompson Jr., R.C., Oegema Jr., T.R., Lewis, J.L., Wallace, L., 1991. Osteoarthrotic changes after acute transarticular load. An animal model. J. Bone and Joint Surg. Am. Vol. 73, 990–1001.

Van der Voet, A.F., Shrive, N.G., Schachar, N.S., 1993. Numerical modelling of articular cartilage in synovial joints: poroelasticity and boundary conditions. In: Middleton, J., Pande, G.N., Williams, K.R. (Eds.), Proceedings of International Conference on Computer Methods in Biomechanics and Biomedical Engineering. IBJ Publishers, pp. 200–209.

Wang, H., Chen, T., Torzilli, P., Warren, R., Maher, S., 2014. Dynamic contact stress patterns on the tibial plateaus during simulated gait: a novel application of normalized cross correlation. J. Biomech. 47, 568–574 (PMCID: 3936672).

Wilson, W., van Donkelaar, C.C., van Rietbergen, B., Huiskes, R., 2005. A fibril-reinforced poroviscoelastic swelling model for articular cartilage. J. Biomech. 38, 1195–1204.

Wilson, W., van Donkelaar, C.C., van Rietbergen, B., Ito, K., Huiskes, R., 2004. Stresses in the local collagen network of articular cartilage: a poroviscoelastic fibril-reinforced finite element study. J. Biomech. 37, 357–366.

Wu, J.Z., Herzog, W., Epstein, M., 1998. Evaluation of the finite element software ABAQUS for biomechanical modelling of biphasic tissues. J. Biomech. 31, 165–169.

Wyler, A., Bousson, V., Bergot, C., Polivka, M., Leveque, E., Vicaut, E., Laredo, J.D., 2009. Comparison of MR-arthrography and CT-arthrography in hyaline cartilage-thickness measurement in radiographically normal cadaver hips with anatomy as gold standard. Osteoarthr. Cartil. 17, 19–25.